

A Photometric Method for Quantifying Asymmetries in Disk Galaxies

David A. Kornreich¹

Center for Radiophysics and Space Research

Martha P. Haynes¹

Center for Radiophysics and Space Research and National Astronomy and Ionosphere Center²

and

R.V.E. Lovelace

Department of Astronomy, Cornell University

ABSTRACT

A photometric method for quantifying deviations from axisymmetry in optical images of disk galaxies is applied to a sample of 32 face-on and nearly face-on spirals. The method involves comparing the relative fluxes contained within trapezoidal sectors arranged symmetrically about the galaxy center of light, excluding the bulge and/or barred regions. Such a method has several advantages over others, especially when quantifying asymmetry in flocculent galaxies. Specifically, the averaging of large regions improves the signal-to-noise in the measurements; the method is not strongly affected by the presence of spiral arms; and it identifies the kinds of asymmetry that are likely to be dynamically important. Application of this “method of sectors” to R -band images of 32 disk galaxies indicates that about 30% of spirals show deviations from axisymmetry at the 5σ level.

Subject headings: galaxies: photometry — galaxies: structure — techniques: photometric

1. Introduction

Traditionally, studies of spiral galaxies have concentrated on understanding the dynamics of axisymmetric disks with simple spiral structure. The high contrast, well-delineated spiral

¹Visiting Astronomer, Kitt Peak National Observatory which is part of the National Optical Astronomy Observatories, operated by the Association of Universities for Research in Astronomy, Inc. under a cooperative agreement with the National Science Foundation.

²The National Astronomy and Ionosphere Center is operated by Cornell University under a cooperative agreement with the National Science Foundation.

structure in ideal “grand design” spiral galaxies is fairly well understood as arising from tidal effects. However, as Baldwin *et al.* (1980) (hereafter BLS) first pointed out, ideal (that is, symmetric) galaxies outside of the grand design class are more uncommon than generally believed. It is now becoming established that perfect symmetry is not nearly as all-pervasive in either visible galaxies or in H I disks as previously assumed.

Asymmetries are generally interpreted (see, for example, Junqueira & Combes 1996) as the excitation and superposition of $m = 1$ spiral modes over the dominant $m = 2$ mode, or as local phase-shifting (with radius) of the $m = 2$ mode initiated by gravitational perturbations due to companion galaxies, even when interacting galaxies are not in evidence. This idea can be extended to include those interactions which result in minor mergers, or gas accretion from the surrounding intergalactic medium, allowing limits to be placed on the total galaxy accretion rate (Zaritsky & Rix 1997, hereafter ZR).

Alternatively, asymmetry in the H I gas velocity field has been interpreted as an indicator of more subtle dynamics occurring within the galaxy itself. It is beginning to be understood that stationary solutions of the hydrodynamics of baryonic and dark matter components may be non-axisymmetric. Shoenmakers *et al.* (1997), for instance, interpret optical asymmetry as an indicator of asymmetry in the overall galactic potential, and therefore an indicator of the (triaxial) spatial distribution of the dark matter in a galaxy. Jog (1997) has studied the orbits of stars and gas in a lopsided potential, and reports that lopsided potentials arising from disks alone are not self-consistent; rather, a stationary lopsided disk must be responding to asymmetries in the halo. Finally, some numerical studies such as that done by Syer & Tremaine (1996) indicate that fluid disks may have non-axisymmetric equilibrium states, even when embedded in an axisymmetric halo.

In certain galaxies, NGC 5474 for example (see van der Hulst & Huchtmeier 1979 and Rownd *et al.* 1994), the center of the optical light is separated from the center of the dynamical H I distribution, possibly indicating that galaxies do not rest in stationary states of the potential at all, but rather that the optical galaxy may be in a libration about the minimum of the the H I or dark matter potential. The preliminary numerical work reported by Levine and Sparke (1998) is suggestive that optical disks offset from dynamical centers can result in intriguing forms of non-axisymmetry.

Several methods have been developed to quantify the frequency of asymmetry in galaxy images. Rix & Zaritsky (1995, hereafter RZ) and ZR analyzed the surface brightness distributions in K' -band images of spiral galaxies. Fourier signal strengths $A_m(r)$ for the m spiral modes were calculated, with large signal strengths (compared to the average surface brightness A_0) indicating asymmetry. RZ concentrated on the $m = 1$ “lopsided” Fourier mode as the primary indicator of asymmetry. Both RZ and ZR conclude that as many as 30% of galaxies show significant deviations from axisymmetry by this measure.

Conselice (1997, hereafter C97) has proposed that asymmetries be measured by a method

in which galaxy images are rotated 180° and subtracted from the original image. Any residuals are interpreted as asymmetries. C97 does not provide error estimates of the derived asymmetry parameter, but comments that in the R -band, at least 54% of 43 sample galaxies have asymmetry parameters $A < 0.1$, where $A = 0$ and $A = 1$ are representative of maximal symmetry and asymmetry, respectively. The observation is also made that galaxies tend to be more asymmetric in the J -band than in the R -band.

Methods for measuring other than global asymmetries have also been proposed. For example, Elmegreen and Elmegreen (1995) study the symmetry of the two dominant inner spiral arms in a sample of 173 bright galaxies. In that study, the relative lengths and positions of the spiral arms were measured and compared. They find that in most galaxies, the inner spiral arm lengths are equal to within 20%, and are within 20° of being 180° apart. Such a method could be extended into the outer regions of a grand design spiral, in lieu of more global methods which can confuse strong spiral structure with asymmetry.

In their study, BLS compared the H I surface density profiles on both sides of the galaxy for a sample of galaxies mapped in H I with sufficient resolution to measure the degree of asymmetry in H I disks. Using a much larger dataset of global H I profiles obtained from the literature, Richter & Sancisi (1994) classified asymmetry qualitatively. Based essentially on differences in the fluxes from the two horns, or total differences in flux between approaching and receding sides, they assigned galaxies to one of three categories of apparent asymmetry: “strong,” “weak,” or no asymmetry. Using the qualitative assignment, Richter & Sancisi concluded that only $47\% \pm 5\%$ of the global profiles show no asymmetry. Furthermore, they argued that an observed correspondence between obviously asymmetric H I maps (such as that for M101) and lopsided line profiles justifies the proposition that an observed asymmetry in the global H I profile can be taken as evidence for a non-circular density distribution. It should be noted, however, that this is a converse argument complicated by the fact that H I profiles contain both velocity field and H I distribution information, which are often difficult to disentangle. Richter & Sancisi did attempt to correct for the presence of companions or the presence of unusual kinematics by eliminating peculiar-looking profiles *a priori*. However, because the H I emission profiles used for this study were taken from observations made with a smorgasboard of telescopes, the effects of pointing error (which could manifest itself as an asymmetry in the profile) could not be determined.

Haynes *et al.* (1998a) have conducted a similar study of H I line profiles in which spectra for a sample of 104 disk galaxies were taken using the 43-meter telescope at Green Bank and examined for asymmetry in a quantitative way. Using two methods for the determination of asymmetry, and after determining that pointing errors produced negligible deviations, the conclusion supported the previous results that asymmetry is found in $\sim 50\%$ of global H I profiles. However, those authors caution that asymmetry in line profiles obtained with single-dish telescopes can arise for a variety of reasons unrelated to disk asymmetry, such as contamination from companions within the main beam or sidelobes.

In this paper, we present a new photometric method for quantifying deviations from axisymmetry in optical images of disk galaxies. Essentially, we attempt to determine the likelihood that the light distribution in a galaxy is inherently symmetric by comparing the relative fluxes received in different directions from the optical center. In §2, we present the observational sample of 32 face-on and nearly face-on galaxies and describe the basic image acquisition and reduction procedures. In §3, the photometric method for the determination of departures from axisymmetry is introduced and then applied to the target sample. Finally in §4, the method is discussed in comparison with other quantitative determinations of asymmetry in spiral disks.

2. Observations

For the purpose of developing a method of measuring departures from axisymmetry, deep *R*-band images were constructed for a set of 32 nearby face-on disk galaxies covering a range of spiral Hubble classes. In this section, we discuss the observational and image reduction procedures for the target sample of galaxies.

2.1. Image Acquisition and Data Reduction

The method of sectors described in the following sections was used to determine differences from symmetry for a sample of 32 face-on disk galaxies listed in Table 1 and displayed in Figure 1. Observations were conducted with a Harris *R*-band filter under nonphotometric conditions. Each galaxy except NGC 3393, NGC 3450, and MCG-5-34-002 was observed with the KPNO 0.9 meter telescope configured to $f/7.5$ and equipped with the T2KA direct imaging camera. The camera setup yielded a gain of 3.6 electrons per adu and a $0''.68$ per pixel scale. Only the inner 1024×1024 pixels were illuminated, resulting in a field of view of $11'.6 \times 11'.6$. Read noise in the camera was 4 electrons per pixel. Observations took place during several observing periods during November and December 1996 and February and March 1997.

The three galaxies NGC 3393, NGC 3450, and MCG-5-34-002 were observed in April 1997 at the CTIO³ 0.9 meter telescope with the T1K2 imaging camera. The gain in this camera is 3.35 electrons per adu and the plate scale is $0''.384$ per pixel at Cassegrain focus. Read noise is 4.6 electrons per pixel.

At both telescopes, individual exposures of 600 seconds each were taken; the total integration time per object was varied depending on the atmospheric transparency.

³The Cerro Tololo Interamerican Observatory is operated by the Association of Universities for Research in Astronomy Inc. (AURA), under a cooperative agreement with the National Science Foundation as part of the National Optical Astronomy Observatories.

Image reduction was accomplished in the *IRAF*⁴ image processing environment. These exposures were then debiased, sky-subtracted, and flatfielded using twilight flats. The exposures were scaled by measuring the integrated fluxes from 5–10 stars in the field. Because the transparency was variable, the frames were scaled to the single frame showing the greatest number of counts regardless of airmass. The frames were then combined using weights inversely proportional to the scale factor used, to produce images with total exposure times of between 3000 and 4800 seconds. Because the images are not photometric (and in some cases, far from photometric), the relation between exposure times and total integration time is not clear. This variability does not affect the measurements conducted here, however, because the interesting quantities involve only magnitude differences of regions within individual images. Estimated errors which involve the integration time, however, may be affected.

After combination, foreground stars were removed from the frame and replaced with a second-order polynomial interpolation of the surrounding background. A record of the number of pixels so replaced was kept, to be used as part of the final error estimate. Elliptical isophotes were then fit to the galaxy using a slightly modified version of the STSDAS⁵ ISOPHOTE package (Haynes *et al.* 1998b). The model galaxy thus obtained was used to determine each galaxy’s center of light, inclination, and disk scale length R_d . Scale length was determined by finding the best fit line in a surface brightness profile for the outer regions of a galaxy. Inclination was estimated under the assumption that galaxies seen face-on should appear circular. This assumption, although widely used to determine inclinations, is suspect in a project wherein inherent circular symmetry is not assumed. It is, however, justified statistically by studies such as that by Binney and de Vaucouleurs (1981) and in RZ, in which the observed distribution of galaxy ellipticities on the sky was used to estimate the distribution of the intrinsic axial ratios of disk and galaxies. We thus take the intrinsic ellipticities of disk galaxies as finite, but well within the errors of our ellipticity measurements. These values and the formal numerical errors are included in Table 1. Following this basic data reduction, images were analyzed for asymmetry using the method of sectors described in the next section.

The images shown in Figure 1 are individually scaled and trimmed for illustrative purposes, and most stars therein are masked to convey the visual appearance of each object.

2.2. The Sample

The observational sample selected for this study was chosen based on applicability for imaging for the purpose of employing the method of sectors discussed in §3. The primary criterion

⁴*IRAF* (Image Reduction and Analysis Facility) is distributed by the National Optical Astronomy Observatories.

⁵STSDAS (Space Telescope Science Data Analysis System) is distributed by the Space Telescope Science Institute which is operated by AURA under contract to the National Aeronautics and Space Administration.

was face-on aspect, to eliminate confusion due to, for instance, the presence of dust lanes and extinction in the disk; the main source was the *Third Reference Catalogue of Bright Galaxies* (de Vaucouleurs *et al.* 1976; RC3). The galaxies in the observed sample were selected based on apparent disk size $1.5 < D_{25} < 5'$, apparent ellipticity $e^* = R_{25} - 1 < 0.15$, and narrow ($W_{HI} \lesssim 100 \text{ km s}^{-1}$) H I line width. The latter restriction is a further diagnostic for low inclination in rotation-dominated disks. Since turbulence contributes to broadening at a level of σ_V (Broeils 1992; Giovanelli *et al.* 1998) $\sim 8 - 15 \text{ km s}^{-1}$ and deviations from coplanar rotation may be quite common (Lewis 1987), H I line widths arising from spirals that are observed to be as narrow as 100 km s^{-1} clearly suggest that the disk is seen face-on. Figure 2 demonstrates how rarely H I line widths are observed to be so narrow. The top panels show the distribution of observed H I line widths W_{HI} for a sample of 3123 galaxies in the Local Supercluster for which H I line widths are available either in the RC3 or, preferentially, in our own private database. Reported velocity widths have been converted to a systematic definition and corrected for instrumental broadening, signal-to-noise and redshift stretch, following Giovanelli *et al.* (1998) and Haynes *et al.* (1998c). The lower three panels show the distributions for spiral subtypes as indicated. Most of the narrow W_{HI} profiles seen in the total sample arise from the low mass dwarf irregular galaxies, whereas only a small percent of spirals, those with inclinations $\leq 15^\circ$, have narrow widths. We have thus used such widths as an important indicator of low inclination.

Because of the desire to understand the nature of departures from symmetry in isolated disks, galaxies with no known nearby companions were preferentially included in the sample. In contrast, NGC 5474, which lies within the gravitational potential of M101 and is well-known for its high degree of asymmetry was included for comparative purposes. Likewise, NGC 1637 was added to the sample because of its well-known optical and infrared asymmetry despite its symmetric H I line profile (see Haynes *et al.* 1998a and Block *et al.* 1994).

Because the observations were conducted during non-photometric conditions when the main program could not be carried out, final target selection was not controlled but rather dependent on the ill-fortune of the primary program. Table 1 lists relevant information about the program objects. Entries in the table are as follows:

Col. 1: Entry number in the Uppsala General Catalog (Nilson 1973), where applicable, or else in our private database, referred to as the Arecibo General Catalog (AGC).

Col 2: NGC or IC designation, or other name, typically from the Catalog of Galaxies and Clusters of Galaxies (Zwicky *et al.* 1960), the ESO-Uppsala Catalog (Lauberts 1982) or the Morphological Catalog of Galaxies (Vorontsov-Velyaminov & Arhipova 1968).

Cols. 3 and 4: Right Ascension and Declination in the 1950.0 epoch, typically from the AGC. In general, the listed positions have $15''$ accuracy.

Col. 5: The morphological type code from the RC3.

Col. 6: The major and minor diameters, D_{25} and d_{25} , in arcmin, from the RC3.

Col. 7: The H I line width, W_{HI} , corrected for instrumental broadening, smoothing, and signal-to-noise, in km s^{-1} . Values are taken from the literature as recorded in the AGC and have been converted with appropriate corrections to the system adopted by Haynes *et al.* (1998c) and Giovanelli *et al.* (1998).

Col. 8: The inclination and its associated error, in degrees, derived from the ellipse fitting procedure described in §2.1, under the assumption of an infinitely thin disk. The errors presented are formal numerical errors derived from constraints on geometrical quantities associated with the isophotes, including position angle and ellipticity. Because the galaxies are so nearly face-on, uncertainties in position angle are typically large. We therefore believe that the presented errors are overestimates.

Col. 9: The heliocentric systemic velocity, V_{\odot} , in km s^{-1} , from the AGC.

Col. 10: The total exposure time of the combined R -band image. Note that the images were all obtained under non-photometric conditions of differing transparency. As discussed in §2.1, some compensation for the variation in conditions was made by varying the total exposure times and by weighting each exposure in forming the combination by the inverse of its scale factor.

While the sample size is too small to treat its completeness, it was compared to the larger sample of all spiral galaxies of distance $cz < 3000 \text{ km s}^{-1}$ in the RC3 with observed values of D_{25} and R_{25} , with the subsample thereof including only those “face-on” galaxies with $R_{25} < 1.3$, and with the subsample comprised of those face-on galaxies within 2000 km s^{-1} . The distributions of several parameters were examined for each sample and mean values obtained. For a thorough investigation into the completeness of the catalogue, and distributions of parameters in the Local Supercluster, see Roberts & Haynes (1994). The parameters examined were: the apparent optical diameter D_{25} , the apparent axial ratio R_{25} , corrected bolometric magnitude B_T^o , $B-V$ and $U-B$ colors, mean surface brightness m'_e , heliocentric velocity, and type index. The analysis indicates that the sample galaxies, with $\langle D_{25} \rangle = 3'.66 \pm 0'.9$, are larger on the sky than on average for the supercluster ($\langle D_{25} \rangle = 2'.12 \pm 1'.0$). The mean $B-V$ and $U-B$ colors and surface brightness of the sample are those of the local supercluster to within errors. The sample spans the spiral sequence with a mean type of Sc. While the sample is in no way complete, it is nonetheless representative of face-on galaxies within the Local Supercluster.

3. The Method of Sectors

We wish to construct a quantitative method for determining when a galaxy disk differs significantly from axisymmetry. We have decided on a method which is geometrically based, provides a global measure of asymmetry, and is applicable to a wide variety of data sets.

The chosen method quantifies departures from disk axisymmetry by dividing the galaxy into a number of equal-area trapezoidal “wedges” in which photometry is to be performed (see Figure

3). The wedges are derived from a series of triangles, with the apex of each located at the center of light of the galaxy. The lateral boundaries of each wedge are radials emanating from this center. Each triangle is then truncated at a predetermined radius near the bulge, and extended outwards to the edge of the visible galaxy, thus creating a trapezoidal section. For most galaxies in the sample, inner and outer boundaries of R_d and $5R_d$ were chosen to ensure that the analysis would not be affected by the bulge component, especially including asymmetries introduced by bars, while including as much of the disk luminosity as possible. When the galaxy under consideration is slightly inclined, the sector pattern can be projected to the appropriate angle of inclination, generally 15° or 30° . Photometry is conducted in each of the sectors, and the magnitude of each sector is compared to that of the others. The magnitude difference between sectors i and j is $\Delta M_n^{ij} \equiv |M_i - M_j|$, and the largest magnitude difference between sectors is ΔM_n^{max} , where n represents the number of sectors used. ΔM_n^{max} is the quantitative measure of asymmetry, and where this quantity is significantly different from zero, this is taken as a detection of such.

To ensure that the method was sensitive to asymmetries in the visible flux, the method was tested by considering the very asymmetric galaxy NGC 5474 (Figure 4). This galaxy contains a nucleus which is so offset from the disk structure as to be disconnected from it. It does, however, have a roughly north–south line of approximate reflection symmetry. Using 6 sectors in a configuration aligned with the line of symmetry, we performed photometry in the sectors and determined the greatest difference between segments was $\Delta M_6^{max} = 2^m14$ magnitudes. Because the sectors were aligned with the line of symmetry, we expected complimentary sectors to have similar total magnitudes. In this test, complimentary sectors across the line of symmetry differed only by an average of $\Delta M_6^c = 0^m15$ magnitudes. Similar results were obtained when the sector boundaries were allowed to vary away from perfect alignment with the symmetry axis by 5° , and for sets of 8 and 10 sectors, with average complimentary sector differences being $\Delta M_8^c = 0^m20$ and $\Delta M_{10}^c = 0^m23$, respectively. The maximum magnitude differences in these cases were $M_8^{max} = 2^m34$ and $M_{10}^{max} = 2^m36$, consistent with ΔM_6^{max} to within the values of ΔM^c .

Errors in the measured flux of a region were estimated as the sum of two distinct factors. The first of these is the formal measurement error in the flux $\delta\sigma$ including both the expected read noise and Gaussian sky noise. The second factor represents uncertainties in the masking of foreground stars. These two errors were added in quadrature for each galaxy to obtain an error estimate in the flux, and then transformed via the usual relations to a final error estimate in the magnitudes.

The most ideal measure of the errors associated with this method would be to perform photometry on the sky in each frame, using the same sector pattern as used on the galaxy. The image frames, however, were generally not large enough to permit this. In order to understand the magnitude of the errors involved, therefore, the method of sectors was applied to a symmetric calibrator galaxy. For this calibration, it was important to choose a symmetric, flocculent disk galaxy so that neither spiral structure nor the presence of strong H II regions would contribute disproportionate amounts of luminosity to any one wedge. For these reasons, the galaxy MCG-1-60-011 was selected. Although classified as Sd in the RC3, this galaxy exhibits rather

tightly wound, very symmetric flocculent spiral structure and exhibits few H II regions.

Observed values of the maximum flux difference Δf^{max} for MCG-1-60-011 were interpreted as 1σ errors away from perfect symmetry in the fluxes. Furthermore, formal errors $\delta\sigma$ were calculated for each flux determination. If ρ_{mask} is the density of masked pixels in the image, and A is the area of a sector, then the errors associated with masking should be proportional to $A\rho_{\text{mask}}$. We therefore introduce the proportionality constant β , such that when added in quadrature, the total error estimate becomes

$$\sigma = \sqrt{\delta\sigma^2 + \beta^2 A^2 \rho_{\text{mask}}^2}. \quad (1)$$

If the Δf^{max} values obtained for this galaxy are truly representative of symmetry, then we expect them to be of order σ . Setting $\sigma = \Delta f^{max}$ *a priori*, it is possible to obtain a value of β for each segment size used. We find β to be roughly constant over segment size, thus the proposition of using Δf^{max} for the estimates of the errors is justified. A value of $\beta = 92.3$ ADU-pixel was taken for use with the remainder of the sample, as this is the average of the three values, none of which vary from the mean value by more than 5%.

Table 2 contains the measured values of ΔM^{max} for the 32 galaxies in the sample with 1σ errors. Each galaxy was studied using three segment patterns consisting of 6, 8, and 10 sectors. Using a larger number of segments effectively compares smaller portions of the galaxy than when fewer segments are used, but in this regime, the estimated errors tend to increase. For the galaxies more than 5σ away from symmetric, we have included the type of asymmetry seen based on the location of the minimum and maximum flux segments in the 8-segment runs. When the extreme segments are adjacent to one another, we designate the galaxy “bisymmetric.” When the extreme segments form a 135° or 180° angle, we call the galaxy “lopsided.” Otherwise, the extreme segments form a 90° angle and the galaxy is “boxy.”

Of a total of 32 galaxies, 10 (31%) are asymmetric at the 5σ level, while 19 (59%) are asymmetric at the 3σ level, where “asymmetric” is taken to mean $\Delta M^{max} > 0$ at the stated confidence level in at least one trial. Because the values of ΔM^{max} are positive definite, however, it is important to note that any given measurement is more likely to be an overestimate than an underestimate of the “true” asymmetry. We therefore prefer to use the 5σ values to report that approximately 30% of nearby field galaxies are optically asymmetric. This result agrees with the estimate found by RZ and ZR.

Standard error estimates as described above could not be applied to NGC 5474, because the galaxy is so asymmetric that all attempts at isophotal ellipse fitting failed. Due to the similarities between the error estimates obtained with MCG-1-60-011 and the ΔM^c values obtained for NGC 5474, we adopted ΔM_n^c as the error estimates for that galaxy. If anything, these are probably overestimates.

4. Discussion

As illustrated in Table 2, the degree of asymmetry returned by the method of sectors agrees roughly with a qualitative eyeball judgment of asymmetry for each galaxy. The only truly deviant result was obtained from NGC 1073, which while qualitatively only slightly asymmetric, returns a very significant ($\simeq 28\sigma$) deviation from symmetry. We believe that this result is due the fact that although the galaxy appears relatively symmetric in the disk, the nucleus is offset from the center of the bar by about $10''$ to the northeast. It should be noted also that this galaxy exhibits a separate region of greatly enhanced surface brightness along the bar. Although this region did not formally affect the measurements, it emphasizes the fact that the bar region of NGC 1073 is peculiar. Such an offset of the nuclear region manifests itself as a strong lopsided asymmetry.

In order to determine whether asymmetric galaxies share any other common characteristics, the subsample of the nine galaxies found to differ from symmetry by at least 5σ (except for NGC 1073 and the peculiar galaxy NGC 5474) was compared to the overall sample of 32 galaxies. If we consider SAB galaxies to have .5 of a bar, then the average “barredness” of the asymmetric galaxies is about 0.44, compared to 0.53, the average “barredness” of the overall sample. We therefore find that lack of symmetry is about evenly distributed between barred and unbarred galaxies. The average morphological type of the asymmetric sample is Sbc.

We also report on the dispositions of the five galaxies which were studied both by ZR and the current work. These galaxies are: NGC 600, NGC 991, NGC 1302, NGC 7742, and MCG-5-34-002 (also known as ESO 446 G 031). Of these five galaxies, RZ and ZR find that all but NGC 991 and MCG-5-34-002 have values of $\langle A_1 \rangle < 0.2$, which they interpret as indicative of overall symmetry. MCG-5-34-002 is reported to have a value $\langle A_1 \rangle = 0.210 \pm 0.021$. As stated in ZR, $\langle A_1 \rangle$ measurements are biased upwards, especially for small $\langle A_1 \rangle$, so this measurement is not inconsistent with symmetry. These findings agree with the current work, in which only NGC 991 is found to be different from symmetric by more than 5σ .

We also examine the galaxies in both our sample and the sample of C97. These galaxies are: NGC 3596, NGC 3631, NGC 4136, and NGC 5701, which in the latter study are given R -band asymmetry parameters of 0.10, 0.12, 0.14, and 0.054 respectively. Although C97 does not provide a “cut-off” value for the asymmetry parameter $A(R)$, we can see in that study that values range from $A(R) = 0$ for the most symmetric galaxies to about $A(R) = 0.16$ for the most asymmetric. Our data are roughly consistent with that of C97, in that we find that the former three galaxies are asymmetric and the latter is symmetric.

It is interesting to note also that global asymmetry may not necessarily be correlated with asymmetry in the inner regions, as measured by Elmegreen and Elmegreen (1995). Even the strongly asymmetric galaxy NGC 1637 is reported to have an inner arm length difference of only 23%, and an arm position difference of only 20° , a result only slightly above the median in both cases.

The method of sectors has advantages over other methods in that it is neither dependent on assumed dominant even spiral modes, nor is it particularly sensitive to small deviations in inclination, which may manifest themselves in the magnitude of the $m = 2$ mode. This is not only because the sectors can be modified to account for slight inclinations, but also because even if the sectors are not modified, a slight deviation δi in inclination will be detected as a slight decrease in the magnitude of sectors along the minor axis only of order $2.5 \log(\cos(\delta i))$. This error is negligible if $2.5 \log(\sin(\delta i)) < 0.1$ for most galaxies, requiring $\delta i \lesssim 25^\circ$. This method also, because of its purely geometric nature, is well suited to find asymmetries other than the $m = 1$ “lopsided” type. Galaxies shaped like dumbbells, or with “boxy” or “triangular” shapes, which although asymmetric may be cut into equally luminous halves, would also be detected with this method.

The method of sectors is suited both to the study of flocculent galaxies, and of galaxies with strong spiral arms, so long as those arms extend around the entire galaxy. This is because the integration over large sections tends to “wash out” effects of the spiral arms which might be seen as asymmetries in the Fourier method of RZ, for instance. We believe that this is a desirable effect, since we would not wish to detect symmetric spiral structure as an asymmetry.

The method of sectors is also applicable to cases where the radially-dependant Fourier method is inapplicable or fails. The philosophy of the methods of RZ and C97 seems to be that the only truly symmetric galaxy is one where the surface brightness is a function of r alone. We believe that this definition ignores the central characteristic of disk galaxies, i.e. that they possess spiral arms, and even $m = 1$ spirals are not in general considered by observers to be qualitatively asymmetric. Thus these two methods would misclassify obviously symmetric, but predominantly one-armed spiral galaxies such as NGC 2326 (Figure 6) as lopsided. We therefore prefer to define symmetry based on equality of total integrated flux in various directions outward from the bulge. The method of sectors is designed to distinguish exactly such symmetry.

Moreover, while the Fourier method is relatively easily applied to optical data from large nearby galaxies, it becomes progressively buried in noise as the data become more scarce. Such a method is not likely to be applicable to, for example: distant galaxies in the optical, HI synthesis data, or output of numerical modeling. The sector method does not suffer nearly as much from undersampling and allows direct comparison of optical photometry to other less prolific data sets. Often, numerical work is presented “as is,” with few quantitative measures available to compare numerical results to actual data. In this regard, because of its use of flux integration over large regions, the method of sectors is easily adaptable to measurements of computer-generated data, allowing direct, quantitative comparison to natural phenomena. In the future, this method will be applied to aperture synthesis H I line mapping data and the results of numerical simulations of a subsample of the galaxies observed here.

This research has been partially supported by NSF grant AST95–28860 to MPH, and AST93–20068 to RVEL, and has made use of the NASA/IPAC Extragalactic Database (NED)

which is operated by the Jet Propulsion Laboratory, California Institute of Technology, under contract with the National Aeronautics and Space Administration. The authors would also like to thank Daniel Dale for acquiring the images obtained at CTIO.

REFERENCES

- Baldwin, J.E., Lynden-Bell, D., & Sancisi, R. 1980, MNRAS, 193, 313. (BLS)
- Binney, J., & de Vaucouleurs, G. 1981, MNRAS, 194, 679.
- Block, D.L., Bertin, G., Stockton, A., Grosbol, P., Moorwood, A.F.M., & Peletier, R.F. 1994, A&A, 288, 365.
- Broeils, A. 1992, Ph.D. Thesis, Univ. of Groningen.
- Conselice, C.J. 1997, PASP, 109, 1251. (C97)
- de Vaucouleurs, G., de Vaucouleurs, A., Corwin, H.G., Buta, R.J., & Paturel, G., 1991. *Third Reference Catalogue of Bright Galaxies* (RC3), University of Texas Press, Austin.
- Elmegreen, D.M., & Elmegreen, B.G. 1995, ApJ, 445, 591.
- Giovanelli, R., Dale, D.A., Haynes, M.P., & Hardy, E. 1998, in preparation.
- Haynes, M.P., Hogg, D.E., Maddalena, R.J., Roberts, M.S., & van Zee, L. 1998a, AJ, 115, 62.
- Haynes, M.P., Giovanelli, R., Salzer, J.J., Wegner, G., Freudling, W.F., da Costa, L.N., Herter, T. & Vogt, N.P. 1998b, in preparation.
- Haynes, M.P., Giovanelli, R., Chamaraux, P. da Costa, L.N., Freudling, W.F., Salzer, J.J. & Wegner, G. 1998c, in preparation.
- Jog, C.J. 1997, ApJ, 488, 642.
- Junqueira, S., & Combes, F. 1996, A&A, 312, 703.
- Lauberts, A. 1982. *The ESO/Uppsala Survey of the ESO (B) Atlas*. European Southern Observatory, Munchen.
- Levine, S.E., & Sparke, L.S. 1998, ApJ, 496, L13.
- Lewis, B.M. 1987, ApJS, 63, 515
- Nilson, P. 1973. *Uppsala General Catalogue of Galaxies*. Uppsala Astron. Obs., Uppsala.
- Rix, H.-W., & Zaritsky, D. 1995, ApJ, 447, 82 (RZ).
- Richter, O.-G., & Sancisi, R. 1994, A&A, 290, L9.
- Roberts, M.S., & Haynes, M.P. 1994, ARA&A, 32, 115.
- Rownd, B.K., Dickey, J.M., & Helou, G. 1994, AJ, 108, 1638.
- Schoenmakers, R.H.M., Franx, M., & de Zeeuw, P.T. 1997, MNRAS, 292, 349.
- Syer, D., & Tremaine, S. 1996, MNRAS, 281, 925.

van der Hulst, J.M. & Huchtmeier, W.K. 1979, A&A, 78, 82.

Vorontsov-Velyaminov, B.A., Archipova, V.P., & Krasnogorskaja, A.A. 1968. *Morphological Catalogue of Galaxies*. Moscow State Univ., Moscow.

Zaritsky, D., & Rix, H.-W. 1997, ApJ, 477, 118 (ZR).

Zwicky, F., Herzog, E., Kowal, C.T., Wild, P., & Karpowicz, M. 1960. *Catalogue of Galaxies and Clusters of Galaxies*. Calif. Inst. Tech., Pasadena. (six volumes)

TABLE 1. Galaxy Sample

UGC/AGC ^a	Other	α (1950)	δ (1950)	Morphology	$D_{25} \times d_{25}$ ''	i^a °	W_{HI} $km s^{-1}$	v_{helio} $km s^{-1}$	t_{exp} s
48	...	000402.0	+473553	Sd	1.51×1.29	31 ± 7	64	4322	3600
410258	N 600 ^b	013035.1	−073409	SB(R')(rs)d	3.31×2.82	15 ± 9	54	1867	3600
420153	N 991 ^b	023304.2	−072214	SAB(rs)c	2.69×2.40	10 ± 11	50	1504	3600
420184	N1042	023756.3	−083850	SAB(rs)cd	4.68×3.63	34 ± 3	97	1373	5400
2193	N1058	024023.2	+370748	SA(rs)c	3.02×2.82	15 ± 4	31	492	4200
2210	N1073	024106.4	+010953	SB(rs)c	4.90×4.47	21 ± 13	53	1211	1800
430170	N1302 ^b	031742.0	−261424	SB(R)(r)0/a	3.89×3.72	19 ± 4	86	1730	5400
440323	N1637	043857.7	−025712	SAB(rs)bc	3.98×3.24	33 ± 4	180	710	4200
450062	MCG-3-14-017	052559.5	−160949	SB(r)b	1.87×1.87	13 ± 22	74	2181	4800
3574	285-010	064855.7	+571426	SA(s)cd	4.17×3.63	29 ± 10	142	1418	5400
3681	N2326	070418.7	+504540	SB(rs)b	1.86×1.78	31 ± 4	...	5985	4800
3685	...	070433.1	+614029	SB(rs)b	3.31×2.75	31 ± 7	74	1797	4200
3826	...	071953.4	+614739	SAB(s)d	3.47×3.02	28 ± 8	52	1733	4200
27532	N3450	104537.7	−203507	SB(r)b	2.51×2.24	22 ± 4	...	3290	4800
27537	N3393	104600.0	−245347	SB(R')(rs)a*	2.19×2.00	25 ± 8	...	3730	4800
6277	N3596	111227.9	+150338	SAB(rs)c	3.98×3.80	26 ± 14	116	1176	3600
6360	N3631	111813.2	+532643	SA(s)c	5.01×4.79	21 ± 8	105	1158	4800
6385	N3642	111925.6	+592101	SA(r)bc*	5.37×4.47	18 ± 5	54	1588	4800
6429	314-025	112225.1	+640011	SA(rs)c	2.09×1.74	22 ± 17	39	3726	2400
6813	N3913	114800.7	+553753	SA(R')(rs)d	2.63×2.57	16 ± 14	29	842	4800
7134	N4136	120645.6	+301218	SAB(r)c	3.98×3.72	20 ± 8	77	609	4800
7961	N4688	124514.0	+043627	SB(s)cd	3.16×2.82	16 ± 21	35	987	1800
9013	N5474	140315.3	+535405	SA(s)c Pec	4.79×4.27	...	33	230	3600
30491	MCG-5-34-002 ^b	141036.0	−292142	SB(s)cd	2.00×1.83	26 ± 7	90	2652	2400
9436	N5701	143641.5	+053450	SB(R)(rs)0/a	4.27×4.07	20 ± 19	118	1556	3600
9915	N5957	153300.9	+121251	SAB(R')(r)ab	2.82×2.63	20 ± 7	88	1827	4200
10020	136-070	154331.7	+204256	Sd	2.14×2.09	14 ± 12	50	2092	4200
11914	N7217	220537.6	+310653	SA(R)(r)ab	3.89×3.24	27 ± 1	304	935	4800
620062	UA428	222136.0	−034400	SB(s)d*	1.91×1.71	34 ± 8	66	2833	5400
630223	MCG-1-60-011	233355.4	−051108	SB(r)d	2.09×1.91	16 ± 5	...	5820	4800
12732	476-106	233809.1	+255730	Sm	3.02×2.82	29 ± 8	100	748	2400
12760	N7742 ^b	234143.1	+102925	SA(r)b	1.70×1.70	11 ± 2	77	1653	4200

^aDisk inclination measured for this paper via isophotal ellipse fitting. (See text.)

^bIncluded in the sample of RZ. (See text.)

TABLE 2. Asymmetries Determined by Sector Comparison

Galaxy	ΔM_6^{max}	ΔM_8^{max}	ΔM_{10}^{max}	asym. by sectors ^a	asym. type ^b	asym. by eye ^c
UGC 48	0.72 ± 0.83	0.67 ± 0.93	0.77 ± 0.96	0.80		none
NGC 600	0.22 ± 0.056	0.28 ± 0.060	0.29 ± 0.064	4.4		sl
NGC 991	0.23 ± 0.039	0.22 ± 0.043	0.27 ± 0.045	5.7	lopsd	mod
NGC 1042	0.24 ± 0.042	0.23 ± 0.047	0.24 ± 0.049	5.2	boxy	mod
NGC 1058	0.28 ± 0.088	0.32 ± 0.097	0.35 ± 0.10	3.3		sl
NGC 1073	0.28 ± 0.014	0.39 ± 0.015	0.58 ± 0.017	27.7	lopsd	sl
NGC 1302	0.11 ± 0.038	0.14 ± 0.044	0.19 ± 0.045	4.0		sl
NGC 1637	0.66 ± 0.046	0.76 ± 0.051	0.79 ± 0.053	14.7	lopsd	str
MCG-3-14-017	0.14 ± 0.16	0.18 ± 0.18	0.21 ± 0.18	1.0		none
UGC 3574	0.55 ± 0.16	0.67 ± 0.18	0.74 ± 0.18	3.8		sl
NGC 2326	0.16 ± 0.11	0.24 ± 0.12	0.24 ± 0.13	1.8		none
UGC 3685	0.49 ± 0.16	0.50 ± 0.18	0.57 ± 0.19	2.9		sl
UGC 3826	0.27 ± 0.27	0.30 ± 0.31	0.37 ± 0.32	1.0		sl
NGC 3450	0.23 ± 0.057	0.29 ± 0.064	0.32 ± 0.068	4.4		mod
NGC 3393	0.28 ± 0.060	0.38 ± 0.066	0.36 ± 0.068	5.2	lopsd	mod
NGC 3596	0.14 ± 0.0090	0.19 ± 0.0096	0.24 ± 0.010	19.8	boxy	mod
NGC 3631	0.18 ± 0.018	0.19 ± 0.020	0.23 ± 0.020	10.3	bis	mod
NGC 3642	0.15 ± 0.062	0.18 ± 0.069	0.22 ± 0.075	2.7		sl
UGC 6429	0.15 ± 0.027	0.16 ± 0.030	0.22 ± 0.032	5.9	lopsd	mod
NGC 3913	0.037 ± 0.35	0.059 ± 0.38	0.066 ± 0.40	0.14		none
NGC 4136	0.12 ± 0.039	0.18 ± 0.043	0.19 ± 0.045	3.8		sl
NGC 4688	0.57 ± 0.045	0.67 ± 0.049	0.68 ± 0.052	13.1	boxy	str
MCG-5-34-002	0.26 ± 0.12	0.33 ± 0.13	0.26 ± 0.14	2.2		none
NGC 5474	2.19 ± 0.75 ^d	2.34 ± 1.00 ^d	2.36 ± 1.15 ^d	...		str
NGC 5701	0.27 ± 0.10	0.28 ± 0.12	0.31 ± 0.12	2.5		none
NGC 5957	0.30 ± 0.066	0.34 ± 0.075	0.35 ± 0.080	4.5		sl
UGC 10020	0.095 ± 0.074	0.15 ± 0.082	0.21 ± 0.085	1.9		none
NGC 7217	0.095 ± 0.067	0.10 ± 0.073	0.11 ± 0.077	1.4		none
UA 428	0.24 ± 0.41	0.34 ± 0.45	0.37 ± 0.47	0.71		none
MCG-1-60-011	0.060 ± 0.062	0.068 ± 0.068	0.074 ± 0.071	1.0		none
UGC 12732	0.19 ± 0.14	0.26 ± 0.16	0.51 ± 0.19	1.9		none
NGC 7742	0.067 ± 0.028	0.097 ± 0.032	0.10 ± 0.033	2.8		none

^aIndicates the detection of asymmetry in units of σ .

^b“lopsided,” “boxy,” or “bisymmetric,” if significantly asymmetric. (see text).

^cIndicates the qualitative appearance of asymmetry in a galaxy as “none,” “slight,” “moderate,” or “strong.”

^dDue to the extreme asymmetry of this galaxy, isophotal ellipses could not be fit. Errors expressed are values of ΔM_n^c , as described in the text.

Fig. 1.— Illustration of the 32 galaxies examined in the current paper and listed in Table 1. Relative sizes and intensities of the images are not to scale.

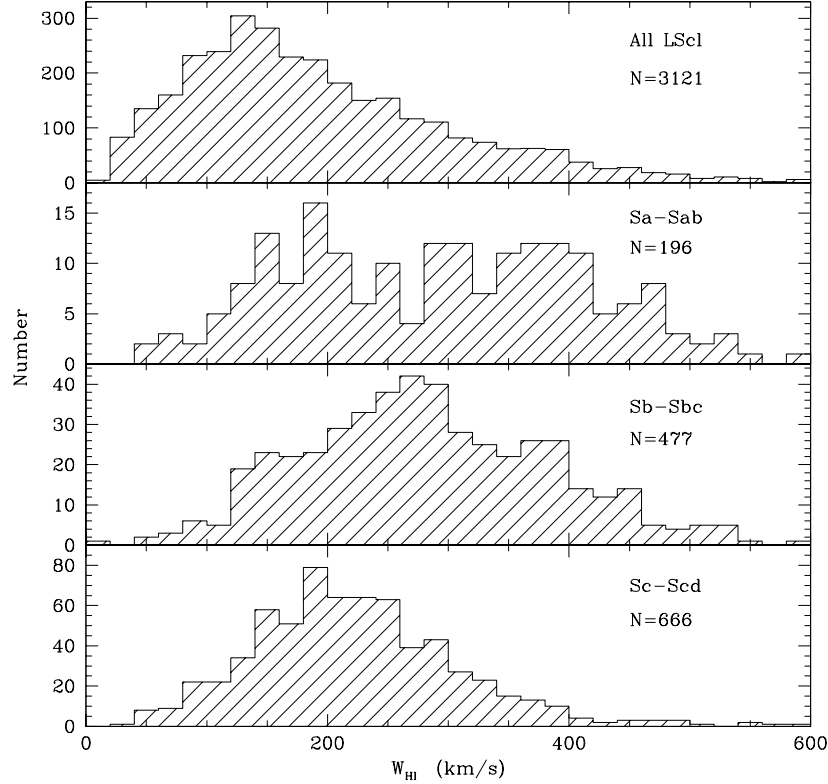


Fig. 2.— HI line width distributions for disk galaxies in the Local Supercluster, by morphological type. Note the small population density with HI line widths less than about 100 km s⁻¹.

Fig. 3.— Illustration of the method used for quantifying asymmetry. Shown are galaxies NGC 1637 (left) and MCG-1-60-011 (right). The galaxy image is sectioned into some number of trapezoidal wedges centered on the nucleus in which photometry is performed. Some galaxies are not precisely face-on; in these cases, so long as the inclination is $i \lesssim 30^\circ$, the sector pattern may be projected to the inclination of the galaxy, as is the case for NGC 1637 above.

Fig. 4.— NGC 5474 with surrounding sector pattern. This galaxy, because of its extreme asymmetry, was used to test the sensitivity of the method of sectors. NGC 5474 lies within the gravitational field of M101, which lies about 1° to the NNW.

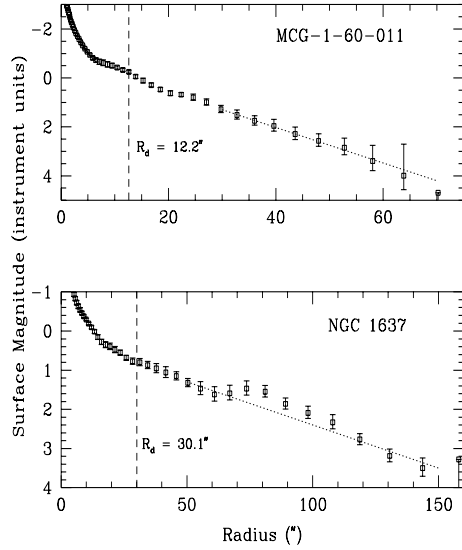


Fig. 5.— The relative surface brightness profile, in instrumental units, for the galaxies MCG-1-60-011 (top) and NGC 1637 (bottom). The dotted line in each panel shows the best linear fit to the outer portions of the profile. The derived disk scale length, R_d , is indicated by the dashed verticals. Each point is associated with an elliptical isophote. The average ellipticity of these isophotes over the region measured with the sector pattern is used to estimate the inclination of the galaxy.

Fig. 6.— The galaxy NGC 2326 exhibits a single spiral arm in the outer regions which can be distinguished for three turns about the nucleus. Due to its strong $m = 1$ spiral mode, such a galaxy would be detected as lopsided with the methods of RZ and C97, but because its integrated luminosity is evenly distributed in θ , it is classified as symmetric by the present method.

This figure "figure1a.jpg" is available in "jpg" format from:

<http://arxiv.org/ps/astro-ph/9807304v1>

This figure "figure1b.jpg" is available in "jpg" format from:

<http://arxiv.org/ps/astro-ph/9807304v1>

This figure "figure3a.jpg" is available in "jpg" format from:

<http://arxiv.org/ps/astro-ph/9807304v1>

This figure "figure3b.jpg" is available in "jpg" format from:

<http://arxiv.org/ps/astro-ph/9807304v1>

This figure "figure4.jpg" is available in "jpg" format from:

<http://arxiv.org/ps/astro-ph/9807304v1>

This figure "figure6.jpg" is available in "jpg" format from:

<http://arxiv.org/ps/astro-ph/9807304v1>